IEEE Access
Multidisciplinary ⋮ Rapid Review ⋮ Open Access Journal

Received 12 February 2024, accepted 23 February 2024, date of publication 7 March 2024, date of current version 21 March 2024.

Digital Object Identifier 10.1109/ACCESS.2024.3374386

RESEARCH ARTICLE

Control Synthesis of Nonholonomic Mobile Robots Under Time-Varying Delays and Input Saturation: Experimental Validation

ANTONIO GONZÁLEZ-SORRIBES, RAFAEL CARBONELL, ANGEL CUENCA, AND JULIAN SALT

Instituto de Automática e Informática Industrial, Universitat Politècnica de València, 46022 Valencia, Spain

Corresponding author: Antonio González-Sorribes (angonsor@upv.es)

This work was supported in part by MCIN/AEI/10.13039/501100011033 under Grant PID2020-116585GB-I00 and Grant PRE2019-088467, in part by "ESF Investing in Your Future," and in part by "Vicerrectorado de Investigación de la Universitat Politècnica de València" under Grant PAID-11-23.

ABSTRACT This paper presents a new control synthesis methodology for nonholonomic mobile robots subjected to time-varying delays and input saturation constraints. The proposed control method is based on smooth static nonlinear functions, leading to a simpler structure than other available control strategies for this class of systems. In addition, the convergence to a certain target position with guaranteed exponential decay rate can be proved for any orientation error. To this end, a nonlinear Lyapunov-Krasovskii functional has specifically been designed to deal with the inherent discontinuity of the kinematics model as well as the presence of time-varying delays. Thus, the control design can efficiently be addressed by means of Linear Matrix Inequalities (LMIs). Finally, the effectiveness of the proposed control design algorithm is validated through simulation and experimentally using a two-wheeled mobile robot.

INDEX TERMS Time delay systems, control synthesis, nonholonomic mobile robot, Lyapunov-Krasovskii functional, linear matrix inequalities.

I. INTRODUCTION

The control synthesis applied to nonholonomic robotic systems is a challenging problem due to their complex nature. Indeed, this class of systems are not controllable (linearly) around the equilibria [1]. Hence, smooth-feedback stability conditions for any initial orientation error cannot be ensured, as discussed in [2]. This fact motivated the design of discontinuous control strategies, such as sliding mode control [3], [4], [5], backstepping control [6] or adaptive control [7], [8], among others. However, these control methods may lead to undesirable phenomena, such as chattering effects and high frequency oscillations as well as high complexity. To circumvent such drawbacks, other proposals resorted to smooth control laws under Takagi-Sugeno fuzzy models and parallel distributed compensation (PDC) in [9]. In this case, the discontinuities and nonlinear terms in the kinematics model were treated by means of sector nonlinearity approach [10] in order to find global stabilizing conditions based on LMIs. However, the main drawback is that only local stability can be proved around the zero-orientation error.

It is noteworthy that many control applications involving nonholonomic mobile robots are subjected to time delays [1] and input saturation constraints [11]. The presence of delays or input saturation in the control loop may lead to poor performance or instability if they are not taken into account in control synthesis [12]. The infinite-dimensional nature of time delay systems prevents from the use of classical techniques to deal with stability analysis. Instead, the Lyapunov-Krasovskii (LK) method [13], [14] allows to prove the stability analysis of time delay systems by checking a *finite* number of Linear Matrix Inequalities (LMIs) [15], which can efficiently be solved using commercially available semidefinite programming tools, such as SeDuMi [16] or LMI Toolbox [17] at the expense of extra conservatism in the worst-case delay estimation. Motivated by this, many efforts have been addressed to reduce such conservatism,

The associate editor coordinating the review of this manuscript and approving it for publication was Ming Xu.

ranging from the construction of more sophisticated LK functionals [18] and the improvement of the integral bounding techniques based on the Jensen's inequality [19] to other more advanced bounding approaches, such as Wirtinger's inequality [20], auxiliary based-functions inequalities [21] or Bessel-Legendre inequalities [22], together with The Reciprocically Convex Lemma [23] to deal with time-varying delays. Other extensions of these methods to nonlinear systems subjected to time-varying delays and input saturation constraints can be found in [24] with nonlinear functions satisfying Lipschitz conditions.

The Lyapunov-Krasovskii method [1], [25], [26] has also been applied for stabilization of nonholonomic systems subjected to time delays. Nevertheless, the latter control strategies involve high nonlinear dynamic equations which are difficult to apply in practice. Considering that the control code programmed at the mobile robot should be kept as simple as possible because of the hardware capabilities limitations [27], the research of easy-to-implement control algorithms is of practical interest [28]. Moreover, in spite of the practical importance of considering input saturation constraints in control synthesis of mobile robots owing to the limited capacities of actuators [11], [29], [30], to the best of the authors' knowledge there are no previous results that simultaneously consider input saturation and time-varying delays for nonholonomic systems.

Motivated by this, the objective of this paper is threefold: (i) design a smooth control strategy for nonholonomic robots subjected to time-varying delays and input saturation constraints, (ii) give a theoretical proof of the exponential convergence to the target position for any orientation error, and (iii) provide experimental results to support the validity of the theoretical conclusions. Hence, the main contributions can be summarized as follows:

- The proposed control law resorts to smooth nonlinear static functions, which is of simpler structure and less complexity than other available strategies, such as those based on sliding mode control [3], [4], [5], backstepping control [6] or adaptive control [7], [8].
- The exponential convergence with guaranteed decay rate under time-varying delays and input saturation constraints is proved via Lyapunov-Krasovskii and LMIs for any initial orientation error.
- The effectiveness of the proposed control synthesis is experimentally validated in a two-wheeled mobile robot in the sense to reduce to the greatest extent the time required to reach the target position (settling time) for a given worst-case delay.

The rest of the paper is organized as follows: Section II describes the problem statement and the proposed control strategy. Section III presents the main results consisting of the LMIs for global exponential stability analysis. Section IV depicts some simulation results, which are experimentally validated in Section V. Finally, some conclusions are gathered in Section VI.

II. PROBLEM STATEMENT

Consider the following kinematic model for a nonholonomic mobile robot (see Fig. 1):

$$\begin{aligned} \dot{x} &= sat(v^{(h)})\, cos(\theta), \\ \dot{y} &= sat(v^{(h)})\, sin(\theta), \\ \dot{\theta} &= sat(w^{(h)}) \end{aligned} \tag{1}$$

where

$$sat(v^{(h)}) = \begin{cases} -\bar{v} & \text{if } v^{(h)} \le -\bar{v} \\ v^{(h)} & \text{if } -\bar{v} < v^{(h)} < \bar{v} \\ \bar{v} & \text{if } v^{(h)} \ge \bar{v} \end{cases},$$
$$sat(w^{(h)}) = \begin{cases} -\bar{w} & \text{if } w^{(h)} \le -\bar{w} \\ w^{(h)} & \text{if } -\bar{w} < w^{(h)} < \bar{w} \\ \bar{w} & \text{if } w^{(h)} \ge \bar{w} \end{cases} \tag{2}$$

being $v^{(h)} \equiv v(t - h(t))$ and $w^{(h)} \equiv w(t - h(t))$ the control actions corresponding to the linear and angular velocities with the saturation constraints $\bar{v}$ and $\bar{w}$ respectively. Both control actions are subjected to a time-varying input delay $h(t)$ satisfying $h_1 \le h(t) \le h_2$ for some scalars $0 \le h_1 \le h_2$. Let (x_r, y_r) be a prescribed reference 2D position to be reached, and:

$$\begin{aligned} \rho &= \sqrt{(x - x_r)^2 + (y - y_r)^2}, \\ \phi &= atan2(y - y_r, x - x_r). \end{aligned} \tag{3}$$

Remark 1: The function $atan2 : \mathcal{R}^2 \to (-\pi, \pi)$ is equivalent to a four-quadrant arctangent function [31] defined as:

$$atan2(y, x) = \begin{cases} 0 & \text{if } (x, y) = (0, 0) \\ arctg\left(\frac{y}{x}\right) + \frac{\pi}{2} sign(y)\,(1 - sign(x)) & \text{otherwise} \end{cases} \tag{4}$$

where

$$sign(a) = \begin{cases} 1 & \text{if } a \ge 0 \\ 0 & \text{otherwise} \end{cases} \tag{5}$$

Applying the above definitions, system (1) can be expressed in polar coordinates as:

$$\begin{aligned} \dot{\rho} &= sat(v^{(h)})\, cos(\phi - \theta), \\ \dot{\phi} &= -\frac{sat\left(v^{(h)}\right)}{\rho} sin(\phi - \theta), \\ \dot{\theta} &= sat(w^{(h)}) \end{aligned} \tag{6}$$

Taking into account the existing trade-off between settling time and tolerance against delays, the objective is to design the control laws for v and w in such a way that the mobile robot can reach the reference position (x_r, y_r) in a certain time interval, while enlarging the worst-case delay as far as possible without reaching the input saturation levels $\bar{v}$ and $\bar{w}$

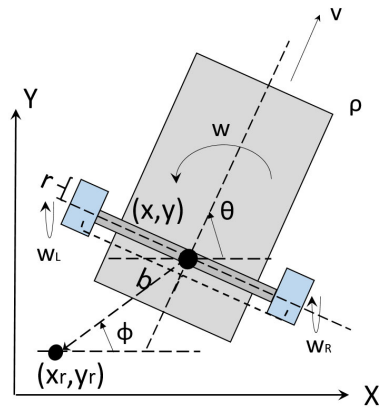

FIGURE 1. Nonholonomic mobile robot: control position system.

respectively. For this purpose, let us consider the following control laws for v and w:

$$v = -K_v \rho \, cos(\phi - \theta),$$
$$w = -K_w sin(\phi - \theta) \tag{7}$$

where K_v, K_w are control gains to be designed.

III. STABILITY ANALYSIS

This section addresses the stability analysis of the closed-loop system formed by (6) and the control law (7). Before proceeding, let us present the following definition, useful later for Theorem 1:

Definition 1 ([32]): The position error $(x - x_r,\ y - y_r)$ in (1) is globally exponentially stable with decay rate α in the sense of the orientation error $\phi - \theta$ if there exists a constant $F(t_0)$ for any $t_0 \geq 0$ such that $\rho \equiv \rho(t) \leq F(t_0)\rho(t_0)e^{-\alpha(t-t_0)}, \forall t \geq t$, regardless of the values of the angles ϕ, θ given in (3).

The fulfilment of the LMI conditions given in Theorem 1 below proves the exponential convergence of the mobile robot (6) with the control (7) to the target position (x_r, y_r) for any time-varying delay $h_1 \leq h(t) \leq h_2$ and any orientation error $\phi - \theta$ without exceeding the input saturation level:

Theorem 1: Given $K_v, K_w < \bar{w}$, h_1, h_2, and α, the closed-loop system formed by (1) and (7) is globally exponentially stable in the sense of Definition 1 satisfying $v < \bar{v}$ and $w < \bar{w}$ for any initial distance to the target position $\rho_0 < \bar{\rho}_0$ if there exist scalars $\gamma_1, \gamma_2, \gamma_3$, symmetric matrices $Q_1, Q_2, R_1, R_4, R_6 \in \mathcal{R}^2, X_1, X_2 \in \mathcal{R}^4, Z_1, Z_2 \in \mathcal{R}^2 > 0$, and matrices $Y_1, Y_2 \in \mathcal{R}^4, R_2, R_3, R_5 \in \mathcal{R}^2 > 0$ satisfying the following LMIs $\forall [i, j, k, m, n, p] = [1, 2] \times [1, 2] \times [1, 2] \times [1, 2] \times [1, 2] \times [1, 2]$:

$$\hat{\Xi}_{ij} + R_1 + h_1^2 R_4 + \tau^2 R_6 + h_1 \left(R_2 + R_2^T\right) + \tau \left(R_3 + R_3^T\right) + h_1 \tau \left(R_5 + R_5^T\right) + h_1 Q_1 + \tau Q_2 < \frac{1}{\bar{\rho}_0^2} I,$$

$$\begin{bmatrix} \Xi_{ij} & \bar{K}_v^T \\ \bar{K}_v & \bar{v}^2 \end{bmatrix} > 0,$$

$$\Xi_{ij} > 0,$$

$$\begin{bmatrix} \hat{\Pi}_{ijkmnp} & \hat{\Pi}_{2,kp}^T \tilde{Z} \\ (*) & -\tilde{Z} \end{bmatrix} < 0,$$

$$\begin{bmatrix} \bar{Z}_2 & 0 \\ 0 & \bar{Z}_2 \end{bmatrix} - (1 - \hat{\delta}_{5n}) \begin{bmatrix} X_1 & Y_1 \\ (*) & 0 \end{bmatrix} - \hat{\delta}_{5n} \begin{bmatrix} 0 & Y_2 \\ (*) & X_2 \end{bmatrix} \geq 0, \tag{8}$$

where

$$\begin{aligned}
\Xi_{ij} &= diag\left(\hat{\Xi}_{ij}, 0, 0\right) + \frac{1}{h_1} diag\,(0, Q_1, 0) \\
&\quad + \frac{1}{\tau} diag\,(0, 0, Q_2) + \bar{R}, \\
\hat{\Xi}_{11} &= I_2 \otimes (\gamma_1 + \gamma_2 + \gamma_3), \\
\hat{\Xi}_{12} &= I_2 \otimes (\gamma_1 + \gamma_2 - \gamma_3), \\
\hat{\Xi}_{21} &= I_2 \otimes (\gamma_1 - \gamma_2 + \gamma_3), \\
\hat{\Xi}_{22} &= I_2 \otimes (\gamma_1 - \gamma_2 - \gamma_3), \\
\hat{\Pi}_{ijkmnp} &= E_1^T \hat{\Pi}_{0,ij} E_1 + He\left(E_1^T \hat{\Pi}_{1,ijmp} E_2\right) \\
&\quad + He\left(\hat{\Pi}_{4,kp}^T \bar{R} \hat{\Pi}_{3,n}\right) + E_1^T Q_1 E_1 - E_3^T Q_1 E_3 \\
&\quad + E_1^T Q_2 E_1 - E_4^T Q_2 E_4 \\
&\quad - \mathcal{D}_1^T \mathcal{W}^T \bar{Z}_1 \mathcal{W} \mathcal{D}_1 - \mathcal{D}_2^T \bar{\mathcal{W}}^T \hat{\mathcal{T}}_n \bar{\mathcal{W}} \mathcal{D}_2, \\
\hat{\Pi}_{2,kp} &= \hat{\Pi}_{21,k} E_1 + \hat{\Pi}_{22,p} E_2, \\
\bar{Z}_1 &= \begin{bmatrix} Z_1 & 0 \\ 0 & 3Z_1 \end{bmatrix}, \bar{Z}_2 = \begin{bmatrix} Z_2 & 0 \\ 0 & 3Z_2 \end{bmatrix}, \\
\tilde{Z} &= h_1^2 Z_1 + \tau^2 Z_2, \quad \hat{\mathcal{T}}_n = \begin{bmatrix} \bar{Z}_2 + \hat{T}_{1,n} & \hat{T}_{2,n} \\ (*) & \bar{Z}_2 + \hat{T}_{3,n} \end{bmatrix}, \\
\hat{T}_{1,n} &= \hat{\delta}_{5n} X_1, \quad \hat{T}_{3,n} = (1 - \hat{\delta}_{5n}) X_2, \\
\hat{T}_{2,n} &= (1 - \hat{\delta}_{5n}) Y_1 + \hat{\delta}_{5n} Y_2, \\
\mathcal{W} &= \begin{bmatrix} 1 & -1 & 0 \\ 1 & 1 & -2 \end{bmatrix} \otimes I_2, \\
\bar{\mathcal{W}} &= I_2 \otimes \mathcal{W}, \qquad \tau = h_2 - h_1.
\end{aligned} \tag{9}$$

being $He(.) = (.) + (.)^T$ for any matrix (.), and

$$\hat{\Pi}_{0,ij} = \begin{bmatrix} \hat{\Omega}_{0,ij} & 0 \\ (*) & \hat{\Omega}_{0,ij} \end{bmatrix}, \quad \hat{\Pi}_{1,ijmp} = \begin{bmatrix} \hat{\Omega}_{1,ijp} & \hat{\Omega}_{2,mp} \\ \hat{\Omega}_{3,ijp} & \hat{\Omega}_{4,mp} \end{bmatrix},$$

$$\hat{\Pi}_{21,k} = \begin{bmatrix} \alpha & \hat{\Omega}_{5,k} \\ 0 & \hat{\Omega}_{6,k} \end{bmatrix}, \quad \hat{\Pi}_{22,p} = \begin{bmatrix} -K_v \hat{\delta}_{6p} & 0 \\ 0 & 0 \end{bmatrix},$$

$$\hat{\Pi}_{3,n} = \begin{bmatrix} E_1^T & h_1 E_5^T & \tau(1 - \hat{\delta}_{5n}) E_6^T + \tau \hat{\delta}_{5n} E_7^T \end{bmatrix}^T,$$

$$\hat{\Pi}_{4,kp} = \begin{bmatrix} \hat{\Pi}_{2,kp}^T & (E_1 - E_3)^T & (E_3 - E_4)^T \end{bmatrix}^T,$$

$$\hat{\Omega}_{0,ij} = \alpha \left(\gamma_1 + \gamma_2 \hat{\delta}_{1i} + \gamma_3 \hat{\delta}_{2j}\right),$$

$$\hat{\Omega}_{1,ijp} = -\frac{1}{2} K_v \hat{\delta}_{6p} \left(\gamma_1 + \gamma_2 \hat{\delta}_{1i} + \gamma_3 \hat{\delta}_{2j}\right),$$

$$\hat{\Omega}_{2,mp} = -\frac{1}{4} K_w \gamma_3 \hat{\delta}_{6p} \hat{\delta}_{4m}, \quad i = 1, 2,$$

$$\hat{\Omega}_{3,ijp} = -\frac{1}{4} K_v \left(\gamma_2 \hat{\delta}_{2j} + \gamma_3 \hat{\delta}_{1i}\right) \hat{\delta}_{6p},$$

$$\hat{\Omega}_{4,mp} = -\frac{1}{4} K_w \gamma_2 \hat{\delta}_{6p} \hat{\delta}_{4m},$$

$$\hat{\Omega}_{5,k} = K_w \hat{\delta}_{3k}, \qquad \hat{\Omega}_{6,k} = \alpha - K_w \hat{\delta}_{3k}.$$

$$\bar{K}_v = \begin{bmatrix} K_v & 0 & 0 & 0 & 0 & 0 \end{bmatrix},$$

$$\bar{R} = \begin{bmatrix} R_1 & R_2 & R_3 \\ R_2^T & R_4 & R_5 \\ R_3^T & R_5^T & R_6 \end{bmatrix},$$
$$E_i = e_i \otimes I_2, \quad i = 1, 2, \ldots, 7,$$
$$e_1 = [1,\ 0,\ 0,\ 0,\ 0,\ 0,\ 0],$$
$$e_2 = [0,\ 1,\ 0,\ 0,\ 0,\ 0,\ 0],$$
$$e_3 = [0,\ 0,\ 1,\ 0,\ 0,\ 0,\ 0],$$
$$e_4 = [0,\ 0,\ 0,\ 1,\ 0,\ 0,\ 0],$$
$$e_5 = [0,\ 0,\ 0,\ 0,\ 1,\ 0,\ 0],$$
$$e_6 = [0,\ 0,\ 0,\ 0,\ 0,\ 1,\ 0],$$
$$e_7 = [0,\ 0,\ 0,\ 0,\ 0,\ 0,\ 1],$$
$$\mathcal{D}_1 = \begin{bmatrix} E_1^T & E_3^T & E_5^T \end{bmatrix}^T,$$
$$\mathcal{D}_2 = \begin{bmatrix} E_3^T & E_2^T & E_6^T & E_2^T & E_4^T & E_7^T \end{bmatrix}^T,$$
$$\hat{\delta}_{11} = \hat{\delta}_{21} = \hat{\delta}_{31} = -1,$$
$$\hat{\delta}_{12} = \hat{\delta}_{22} = \hat{\delta}_{32} = 1,$$
$$\hat{\delta}_{41} = 1, \quad \hat{\delta}_{42} = e^{-\alpha h_2} - 1,$$
$$\hat{\delta}_{51} = 0, \quad \hat{\delta}_{52} = 1,$$
$$\hat{\delta}_{61} = e^{\alpha h_1}, \quad \hat{\delta}_{62} = e^{\alpha h_2}. \tag{10}$$

Proof: See Appendix VI-A. □

Remark 2: From ξ_1, ξ_2 in (14), notice that $\xi_1 = 0$, $\xi_2 = 0$ if and only if $\rho = 0$ for any orientation error $\phi - \theta$. Noting that $\dot{V} < 0$ (43) has a quadratic form with the augmented state vector $\bar{\xi}$ in (40), one can deduce that the fulfilment of the LMI conditions of Theorem 1 implies the global exponential convergence of the position error in the sense of Definition 1. The proposed LKF (Lyapunov-Functional Candidate) V given in (12) has been crucial to this end, allowing to give LMI conditions of Theorem 1 that prove global exponential stability with the proposed smooth control function (7) in spite of the discontinuity of the nonholonomic kinematics model (6). In addition, the structure of V allows to take advantage of the Wirtinger's inequality [20] to reduce the conservatism of the integral inequalities in (27), and the Reciprocally Convex Lemma [23] to deal with time-varying delays in (30).

Remark 3: Note that Theorem 1 cannot be directly used for control design since the controller gains K_v, K_w must be set in advance. From the fact that small values for K_v and K_w usually lead to slow convergence, and high values for K_v, K_w tend to closed-loop instability in the presence of delays or input saturation, it can be seen that there exists an optimal choice for such gains in the sense of maximum worst-case delay whose values can be found by dichotomic search with the aid of Theorem 1, starting from sufficiently small gains.

Remark 4: Note that the above conditions do not require to bound the time-derivative of $\tau(t)$. Hence, arbitrarily fast time-varying delays are allowed. This feature allows to include sampling-based sensors with zero-order hold mechanisms, leading to time-varying delay functions of sawtooth structure with positive unitary slope and discontinuities at each sampling instant. For the case of time-varying delays with known bounded derivative, a new component of the form $\int_{t-h(t)}^{t-h_1} \xi^T(s) Q \xi(s) ds$ for a certain symmetric matrix $Q > 0$ can be included in the LKF proposed in (12) to reduce conservatism. Since the experimental platform includes the effect of sampling period, we have intentionally addressed the case of time-varying delays with unknown time-derivative.

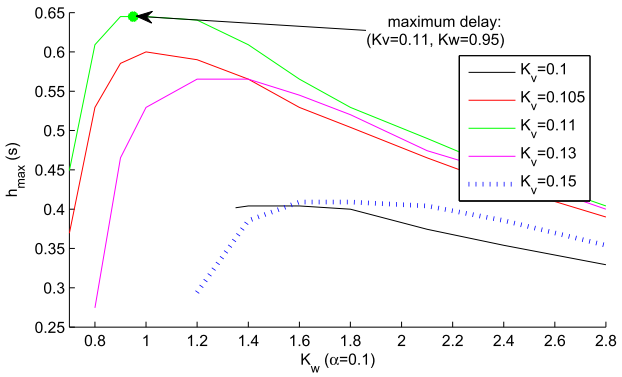

FIGURE 2. Worst-case delay $h_{max} = h_1 = h_2$ as a function of the controller gains K_v and K_w obtained by Theorem 1 for a decay rate $\alpha = 0.1$ and maximum linear and angular velocities of $0.19 m/s$ and $2.82 rad/s$ respectively.

IV. SIMULATION EXAMPLES

Consider a nonholonomic robot with a kinematic model described by (1) and the proposed control law (7). The goal is to design the control gains K_v, K_w in order to reach the target position with prescribed maximum settling time around 30s with error less than 98% (decay rate $\alpha = 0.1$), where the worst-case delay h_2 is enlarged to the greatest extent. Applying Theorem 1 with $\alpha = 0.1$ and $h_1 = h_2$ for different values of K_v, the worst-case delay h_2 is depicted in Fig 2 as a function of K_w. It can be seen that the maximum worst-case delay h_2 is obtained for $K_v = 0.11$ and $K_w = 0.95$ (green solid line in Fig 2).

In order to give a comparison between the control performance with the designed values $K_v = 0.11$ and $K_w = 0.95$ and other choices for K_v, K_w, different simulations have been carried out by means of MATLAB-Simulink and the Simscape Multibody library. A detailed description of the simulation platform can be found in [33]. The obtained results have been depicted in Fig. 3 and Fig. 4. Fig. 3 shows the trajectories in the XY plane described by the mobile robot, and Fig. 4 represents the time evolution of the distance ρ to the target position. The first simulation (red dashed line) has been performed without delays considering the designed values $K_v = 0.11$ and $K_w = 0.95$ (nominal case). Then, the worst-case delay has been increased until $h_2 = 0.9s$. It can be appreciated that the settling time of $30s$ is maintained (green line). The rest of simulations have been carried out choosing other different values for K_v, K_w with $h_2 = 0.9s$. Comparatively, the control gains $K_v = 0.11$ and $K_w = 0.95$ give the fastest response in comparison to other choices: smaller values for the controller gains lead to slower convergence (for instance $K_v = 0.05$, $K_w = 0.95$, blue dashed line), and higher values for the controller gains lead

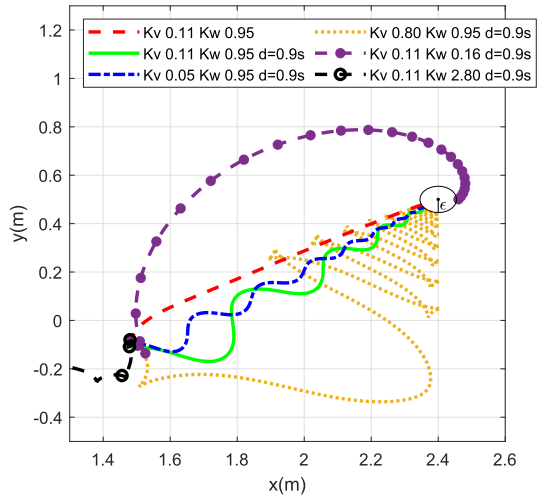

FIGURE 3. Simulation data: comparison of the system trajectories in the XY plane for different control gains K_v, K_w with the designed values $K_v = 0.11$ and $K_w = 0.95$ in the presence of time delays.

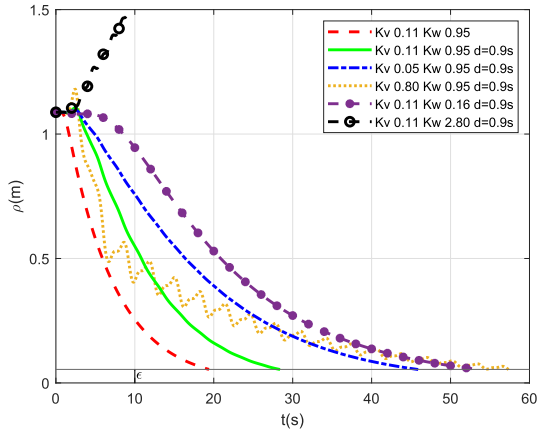

FIGURE 4. Simulation data: comparison of the time-evolution of the distance $\rho(m)$ to the target position for different control gains K_v, K_w with the designed values $K_v = 0.11$ and $K_w = 0.95$ in the presence of time delays.

to undesirable oscillations and even closed-loop instability caused by such delays. The control execution in all cases is forced to stop once the mobile robot is detected to be close to the target position. In Fig. 5, the time evolution of linear and angular velocities (control actions) are depicted for the designed control gains $K_v = 0.11$ and $K_w = 0.95$ considering the non-delayed and delayed case. It can be appreciated that the input saturation level is not reached during control execution, as expected from the two first constraints given in (8) (see Theorem 1).

V. EXPERIMENTAL VALIDATION

Experimental tests were conducted on a physical system to validate the effectiveness of the proposed control synthesis method. The system was implemented using a LEGO platform and Arduino [34] (see Fig. 6). In our case, the mobile robot consists of a nonholonomic system such as depicted in Fig. 1. Two servo systems are implemented to obtain the desired angular speed at each wheel, namely w_L and w_R for

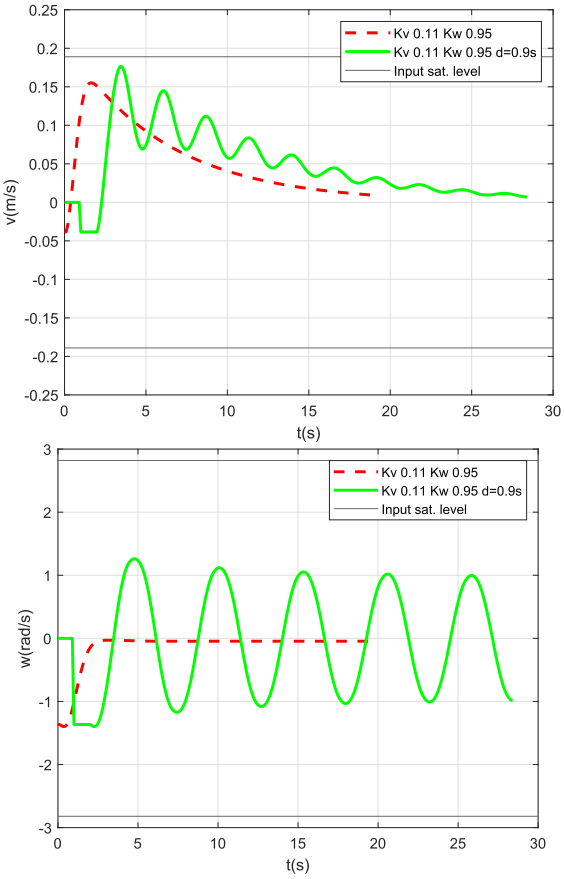

FIGURE 5. Simulation data: time-evolution of linear and angular velocities v, w with the designed values $K_v = 0.11$ and $K_w = 0.95$, together with the input saturation levels.

FIGURE 6. Two-wheeled mobile robot based on LEGO platform and Arduino.

left and right wheels respectively, where $w_L < 13.5 rad/s$ and $w_R < 13.5 rad/s$. The angular velocity control systems for both wheels were adjusted to obtain a settling time around $0.4s$, so their dynamics can be considered to be neglectable. It is easy to see that the angular velocities of left and right

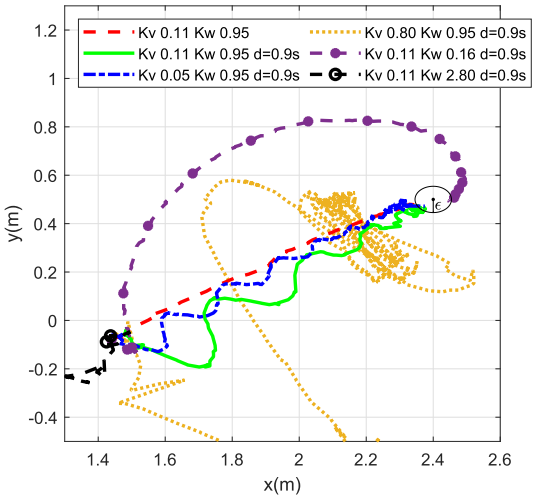

FIGURE 7. Experimental setup: system trajectories in the XY plane for different control gains including $K_V = 0.11$ and $K_W = 0.95$.

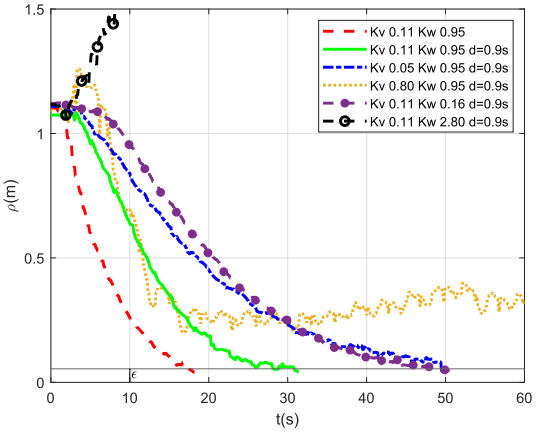

FIGURE 8. Experimental setup: time-evolution of the distance $\rho(m)$ to the target position under different control gains including $K_V = 0.11$ and $K_W = 0.95$.

wheels (w_L, w_R) are related to v, w as:

$$\begin{bmatrix} w_L \\ w_R \end{bmatrix} = \begin{bmatrix} \frac{1}{r} & \frac{b}{r} \\ \frac{1}{r} & -\frac{b}{r} \end{bmatrix} \begin{bmatrix} v \\ w \end{bmatrix}, \tag{11}$$

where r is the wheel radius and b is the length of the axis between them (see Fig. 1). Therefore, neglecting the dynamics of the wheel servo systems, it is easy to see that w_L, w_R can directly be obtained by means of (11) from the proposed control laws w and v in (7). The parameter values for the prototype used in the experimental setup are $r = 0.028m$ and $b = 0.068m$ respectively, and the input saturation constraints are $\bar{v} = 0.19m/s$ and $\bar{w} = 2.82rad/s$. The position (x, y) was measured using Marvelmind Indoor Positioning System [35] at 12 Hz.

The utilization of Arduino as an intermediary between LEGO and Marvelmind facilitates swift code development, as significant portions of the code designed for simulation can be seamlessly transferred to Arduino. However, some challenges arise when certain hardware components that are essential for the practical application are not inherently supported by Simulink. In such cases, additional implementations become necessary to accommodate these requirements, such as integrating beacon readings or establishing communication with LEGO via USART.

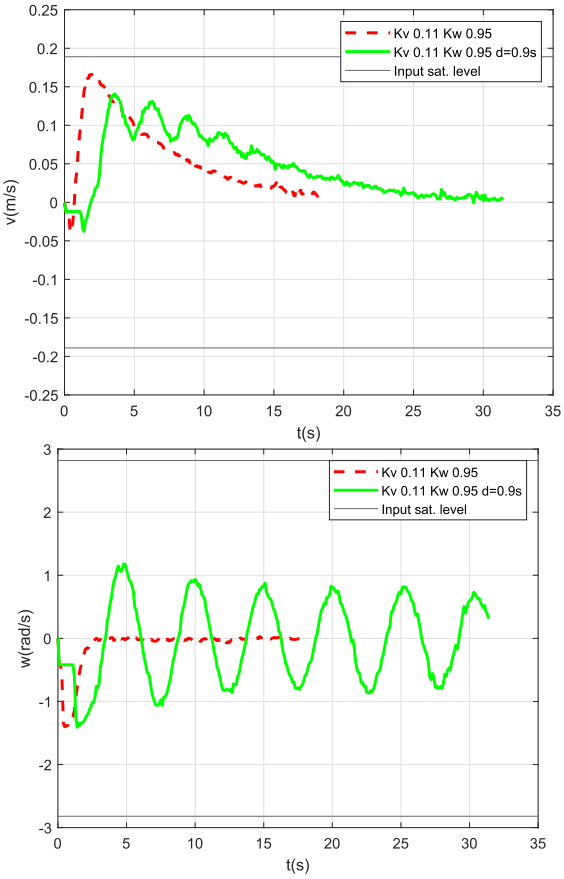

FIGURE 9. Experimental data: time-evolution of linear and angular velocities v, w with the designed values $K_V = 0.11$ and $K_W = 0.95$, together with the input saturation levels.

For validation purposes, extra time-varying delays have been induced by software in order to increase the worst-case delay h_2 until the settling time of $30s$ is slighlty overflowed with the control gains $K_v = 0.11$ and $K_w = 0.95$, which were designed in Section IV. As a result, we obtain that the actual worst-case delay is $h_2 = 0.9$.

The meaning of Fig. 7 and Fig. 8 is respectively the same as Fig. 3 and Fig. 4, but with experimental results. From the figures, one can see that other choices for K_v, K_w give a slower response (if controller gains are smaller), overdamped response, or even instability (if controller gains are greater) in comparison to the designed $K_v = 0.11$ and $K_w = 0.95$. This fact confirms the effectiveness of the control synthesis method. Additionally, the input saturation level is not reached during control execution, as can be deduced from the time evolution of v and w depicted in Fig. 9.

VI. CONCLUSION

This work has presented a simple and low computational cost algorithm for the position control of nonholonomic mobile robots. The exponential convergence with guaranteed decay rate has theoretically been proved for any orientation

error. The key difficulties have been: (i) the construction of a suitable LKF candidate to reach a global exponential stability condition, in spite of the discontinuity of the kinematics model and the use of a smooth control law, (ii) the integration of some recent advances to reduce conservatism in performance analysis under time-varying delays, applied for the first time to nonholonomic systems, and (iii) the inclusion of extra LMI conditions to handle input saturation constraints. Finally, an experimental validation has been provided to show that the proposed method can effectively reduce the settling time to reach the target position in comparison with other choices for a certain worst-case delay.

APPENDIX
PROOF OF THEOREM 1

First, let us define $\rho_\alpha = \rho e^{\alpha t}$ in order to deal with exponential stabilization, where $\alpha \geq 0$ is the decay rate. Then, given some scalars $\gamma_1, \gamma_2, \gamma_3$ and symmetric matrices $Q_1, Q_2 \in \mathcal{R}^2, Z_1, Z_2 \in \mathcal{R}^2 > 0$ and $\bar{R} \in \mathcal{R}^6 > 0$, the following nonquadratic Lyapunov-Krasovskii functional satisfying $V > 0,\ \forall \rho_\alpha > 0, \phi, \theta \in \mathcal{R}$ is proposed:

$$\begin{aligned} V = {} & \frac{\gamma_1}{2}\rho_\alpha^2 + \frac{\gamma_2}{2}\rho_\alpha^2 cos(\phi-\theta) + \frac{\gamma_3}{2}\rho_\alpha^2 sin(\phi-\theta) + \xi_r^T \bar{R}\xi_r \\ & + \int_{t-h_1}^{t} \xi^T(s)Q_1\xi(s)ds \\ & + h_1 \int_{-h_1}^{0}\int_{t+s}^{t} \dot{\xi}^T(g)Z_1\dot{\xi}(g)dgds \\ & + \int_{t-h_2}^{t-h_1} \xi^T(s)Q_2\xi(s)ds \\ & + \tau \int_{-h_2}^{-h_1}\int_{t+s}^{t} \dot{\xi}^T(g)Z_2\dot{\xi}(g)dgds \end{aligned} \tag{12}$$

where $\tau = h_2 - h_1$, $\xi = \begin{bmatrix}\xi_1^T & \xi_2^T\end{bmatrix}^T$, and

$$\begin{aligned} \xi_r &= \begin{bmatrix}\xi^T, & \tilde{\eta}_1^T, & \tilde{\eta}_2^T\end{bmatrix}^T, \\ \tilde{\eta}_1(t) &= \int_{t-h_1}^{t} \xi(s)ds, \quad \tilde{\eta}_2(t) = \int_{t-h_2}^{t-h_1} \xi(s)ds \end{aligned} \tag{13}$$

with ξ_1, ξ_2 defined as

$$\begin{aligned} \xi_1 &= \rho_\alpha cos(\phi-\theta), \\ \xi_2 &= \rho_\alpha sin(\phi-\theta). \end{aligned} \tag{14}$$

The following conditions in V must be satisfied in order to ensure the global exponential convergence with decay rate α: (i) $V > 0$, and (ii) $\dot{V} < 0$ for all possible system trajectories. In addition, the conditions given in subsection VI-C must be satisfied in order not to reach the input saturation level: $v \leq \bar{v}$ and $w \leq \bar{w}$. Hence, the proof is divided into the three corresponding subsections:

A. PROOF OF V > 0

First, let us write V as

$$V = V^* + h_1 \int_{-h_1}^{0}\int_{t+s}^{t} \dot{\xi}^T(g)Z_1\dot{\xi}(g)dgds + \tau \int_{-h_2}^{-h_1}\int_{t+s}^{t} \dot{\xi}^T(g)Z_2\dot{\xi}(g)dgds \tag{15}$$

where

$$\begin{aligned} V^* = {} & \sum_{i=1}^{2}\sum_{j=1}^{2} \mu_{1i}\mu_{2j}\left(\xi_r^T \hat{\Xi}_{ij}\xi_r\right) \\ & + \int_{t-h_1}^{t} \xi^T(s)Q_1\xi(s)ds + \int_{t-h_2}^{t-h_1} \xi^T(s)Q_2\xi(s)ds \end{aligned} \tag{16}$$

and

$$\begin{aligned} \mu_{11} &= \frac{1}{2}(1 + cos(\phi-\theta)), \qquad \mu_{12} = 1 - \mu_{11}, \\ \mu_{21} &= \frac{1}{2}(1 + sin(\phi-\theta)), \qquad \mu_{22} = 1 - \mu_{21}. \end{aligned} \tag{17}$$

with $\hat{\Xi}_{ij}$ defined in (9). Now, applying Jensen's inequalities, one has that

$$\begin{aligned} & \int_{t-h_1}^{t} \xi^T(s)Q_1\xi(s)ds \\ & \geq \frac{1}{h_1}\left(\int_{t-h_1}^{t} \xi^T(s)\right) Q_1 \left(\int_{t-h_1}^{t} \xi(s)\right) \\ & = \frac{1}{h_1}\xi_r^T\left(diag\left(0, Q_1, 0\right)\right)\xi_r, \\ & \int_{t-h_2}^{t-h_1} \xi^T(s)Q_2\xi(s)ds \\ & \geq \frac{1}{h_2-h_1}\left(\int_{t-h_2}^{t-h_1} \xi^T(s)\right) Q_2 \left(\int_{t-h_2}^{t-h_1} \xi(s)\right) \\ & = \frac{1}{h_2-h_1}\xi_r^T\left(diag\left(0, 0, Q_2\right)\right)\xi_r. \end{aligned} \tag{18}$$

Therefore, from (16) and (18), it can be deduced that

$$V^* > \sum_{i=1}^{2}\sum_{j=1}^{2} \beta_{1i}\beta_{2j}\left(\xi_r^T \Xi_{ij}\xi_r\right) \tag{19}$$

where Ξ_{ij} is given in (9). Taking into account that $Z_1, Z_2 > 0$, one can see from (15) that $V^* > 0$ implies $V > 0$. Finally, applying convex sum properties considering that $0 \leq \beta_{f1} \leq 1$, $0 \leq \beta_{f2} \leq 1$, $f = 1, 2$ and $\beta_{1f} + \beta_{2f} = 1$, it can be deduced from (19) that $V^* > 0$ if $\Xi_{ij} > 0, i = 1, 2, j = 1, 2$.

B. PROOF OF V < 0

Time-derivative of V can be obtained as:

$$\begin{aligned} \dot{V} = {} & \gamma_1\rho_\alpha\dot{\rho}_\alpha + \gamma_2\rho_\alpha cos(\phi-\theta)\dot{\rho}_\alpha \\ & - \frac{\gamma_2}{2}\rho_\alpha^2 sin(\phi-\theta)\left(\dot{\phi}-\dot{\theta}\right) \\ & + \gamma_3\rho_\alpha sin(\phi-\theta)\dot{\rho}_\alpha \\ & + \frac{\gamma_3}{2}\rho_\alpha^2 cos(\phi-\theta)\left(\dot{\phi}-\dot{\theta}\right) \\ & + \dot{\xi}_r^T\bar{R}\xi_r + \xi_r\bar{R}\dot{\xi}_r^T \\ & + \xi^T(t-h_1)Q_1\xi(t-h_1) - \xi^T Q_1\xi \\ & + \xi^T(t-h_2)Q_2\xi(t-h_2) - \xi^T(t-h_1)Q_2\xi(t-h_1) \\ & + h_1^2\dot{\xi}^T Z_1\dot{\xi} - h_1\int_{t-h_1}^{t} \dot{\xi}(s)^T Z_1\dot{\xi}(s)ds \end{aligned}$$

$$+\tau^2\dot{\xi}^T Z_2\dot{\xi} - \tau\int_{t-h_2}^{t-h_1}\dot{\xi}(s)^T Z_2\dot{\xi}(s)ds \tag{20}$$

From the definition of $\rho_\alpha = \rho e^{\alpha t}$, the time-derivative renders

$$\dot{\rho}_\alpha = \dot{\rho}e^{\alpha t} + \alpha\rho_\alpha = sat(v^{(h)})e^{\alpha t}\,cos(\phi-\theta) + \alpha\rho_\alpha. \tag{21}$$

The fulfilment of the two first inequalities given in (8) implies that the input saturation level is never reached, that is to say, $v < \bar{v}$ and $w < \bar{w}$, as proved later in Section VI-C. Hence, we have that:

$$sat(v^{(h)}) = v^{(h)}, \qquad sat(w^{(h)}) = w^{(h)}. \tag{22}$$

Hence, replacing $\dot{\rho}_\alpha$ from (21), together with $\dot{\phi}$, $\dot{\theta}$ from (6) into the above expression, and taking into account (22), one has that:

$$\begin{aligned}
\dot{V} &= \gamma_1\rho_\alpha v^{(h)}e^{\alpha t}cos(\phi-\theta) + \gamma_1\alpha\rho_\alpha^2 \\
&+ \gamma_2\rho_\alpha v^{(h)}\,e^{\alpha t}cos^2(\phi-\theta) + \gamma_2\alpha\rho_\alpha^2 cos(\phi-\theta) \\
&- \frac{\gamma_2}{2}\rho_\alpha^2 sin(\phi-\theta)\left(-\frac{v^{(h)}}{\rho}sin(\phi-\theta) - w^{(h)}\right) \\
&+ \gamma_3\rho_\alpha v^{(h)}\,e^{\alpha t}cos(\phi-\theta)sin(\phi-\theta) + \gamma_3\alpha\rho_\alpha^2 sin(\phi-\theta) \\
&+ \frac{\gamma_3}{2}\rho_\alpha^2 cos(\phi-\theta)\left(-\frac{v^{(h)}}{\rho}sin(\phi-\theta) - w^{(h)}\right) \\
&+ \dot{\xi}_r^T\bar{R}\xi_r + \xi_r\bar{R}\dot{\xi}_r^T \\
&+ \xi^T(t-h_1)Q_1\xi(t-h_1) - \xi^T Q_1\xi \\
&+ \xi^T(t-h_2)Q_2\xi(t-h_2) - \xi^T(t-h_1)Q_2\xi(t-h_1) \\
&+ h_1^2\dot{\xi}^T Z_1\dot{\xi} - h_1\int_{t-h_1}^{t}\dot{\xi}(s)^T Z_1\dot{\xi}(s)ds \\
&+ \tau^2\dot{\xi}^T Z_2\dot{\xi} - \tau\int_{t-h_2}^{t-h_1}\dot{\xi}(s)^T Z_2\dot{\xi}(s)ds.
\end{aligned} \tag{23}$$

From (14) and (7) the following equivalences can be deduced:

$$\begin{aligned}
\rho_\alpha^2 &= \xi_1^2 + \xi_2^2, \\
v^{(h)}e^{\alpha t} &= -K_v\xi_1^{(h)}e^{\alpha h(t)}.
\end{aligned} \tag{24}$$

Taking into account (24) and ξ_1, ξ_2 given in (14), the expression (23) can be rewritten as:

$$\begin{aligned}
\dot{V} &= -K_v\gamma_1 e^{\alpha h(t)}\xi_1\xi_1^{(h)} + \gamma_1\alpha\left(\xi_1^2+\xi_2^2\right) \\
&-K_v\gamma_2\xi_1\xi_1^{(h)}e^{\alpha h(t)}cos(\phi-\theta) \\
&+ \gamma_2\alpha\left(\xi_1^2+\xi_2^2\right)cos(\phi-\theta) \\
&- \frac{K_v\gamma_2}{2}\xi_2\xi_1^{(h)}e^{\alpha h(t)}sin(\phi-\theta) - \frac{K_w\gamma_2}{2}\left(\frac{\rho_\alpha}{\rho_\alpha^{(h)}}\right)\xi_2\xi_2^{(h)} \\
&- K_v\gamma_3\xi_1\xi_1^{(h)}e^{\alpha h(t)}sin(\phi-\theta) \\
&+ \gamma_3\alpha\left(\xi_1^2+\xi_2^2\right)sin(\phi-\theta) \\
&- \frac{K_v\gamma_3}{2}\xi_2\xi_1^{(h)}e^{\alpha h(t)}cos(\phi-\theta) - \frac{K_w\gamma_3}{2}\left(\frac{\rho_\alpha}{\rho_\alpha^{(h)}}\right)\xi_1\xi_2^{(h)} \\
&+ \dot{\xi}_r^T\bar{R}\xi_r + \xi_r\bar{R}\dot{\xi}_r^T \\
&+ \xi^T(t-h_1)Q_1\xi(t-h_1) - \xi^T Q_1\xi \\
&+ \xi^T(t-h_2)Q_2\xi(t-h_2) - \xi^T(t-h_1)Q_2\xi(t-h_1) \\
&+ h_1^2\dot{\xi}^T Z_1\dot{\xi} - h_1\int_{t-h_1}^{t}\dot{\xi}(s)^T Z_1\dot{\xi}(s)ds \\
&+ \tau^2\dot{\xi}^T Z_2\dot{\xi} - \tau\int_{t-h_2}^{t-h_1}\dot{\xi}(s)^T Z_2\dot{\xi}(s)ds.
\end{aligned} \tag{25}$$

The last integral term of the above expression can be decomposed as:

$$\begin{aligned}
\tau\int_{t-h_2}^{t-h_1}\dot{\xi}(s)^T Z_2\dot{\xi}(s)ds &= \tau\int_{t-h_{(t)}}^{t-h_1}\dot{\xi}(s)^T Z_2\dot{\xi}(s)ds \\
&+ \tau\int_{t-h_2}^{t-h(t)}\dot{\xi}(s)^T Z_2\dot{\xi}(s)ds.
\end{aligned} \tag{26}$$

Applying Wirtinger's inequality, the last two integral terms in (25) and (26) can respectively be bounded by:

$$\begin{aligned}
&-h_1\int_{t-h_1}^{t}\dot{\xi}(s)^T Z_1\dot{\xi}(s)ds \le -\chi_1^T\left(\mathcal{W}^T\bar{Z}_1\mathcal{W}\right)\chi_1, \\
&-\tau\int_{t-h_{(t)}}^{t-h_1}\dot{\xi}(s)^T Z_2\dot{\xi}(s)ds \le -\chi_{21}^T\left(\alpha_d(t)\mathcal{W}^T\bar{Z}_2\mathcal{W}\right)\chi_{21}, \\
&-\tau\int_{t-h_2}^{t-h(t)}\dot{\xi}(s)^T Z_2\dot{\xi}(s)ds \le \\
&-\chi_{22}^T\left((1-\alpha_d(t))\mathcal{W}^T\bar{Z}_2\mathcal{W}\right)\chi_{22},
\end{aligned} \tag{27}$$

where $\alpha_d(t) = \frac{h(t)-h_1}{\tau}$, and

$$\begin{aligned}
\chi_1 &= \left[\xi^T(t)\;\; \xi^T(t-h_1)\;\; \tfrac{1}{h_1}\tilde{\eta}_1^T(t)\right]^T, \\
\chi_{21} &= \left[\xi^T(t-h_1)\;\xi^T(t-h(t))\;\tfrac{1}{h(t)-h_1}\tilde{\eta}_{21}^T(s)ds\right]^T, \\
\chi_{22} &= \left[\xi^T(t-h(t))\;\xi^T(t-h_2)\;\tfrac{1}{h_2-h(t)}\tilde{\eta}_{22}^T(s)ds\right]^T,
\end{aligned} \tag{28}$$

where

$$\tilde{\eta}_{21}(s) = \int_{t-h(t)}^{t-h_1}\xi(s), \qquad \tilde{\eta}_{22}(s) = \int_{t-h_2}^{t-h(t)}\xi(s). \tag{29}$$

Applying the Reciprocically Convex Lemma [23], we have that

$$\begin{aligned}
&-\frac{1}{\alpha_d(t)}\chi_{21}^T\mathcal{W}^T\bar{Z}_2\mathcal{W}\chi_{21} - \frac{1}{1-\alpha_d(t)}\chi_{22}^T\mathcal{W}^T\bar{Z}_2\mathcal{W}\chi_{22} \\
&\le -\chi_2^T\bar{\mathcal{W}}^T\mathcal{T}(t)\bar{\mathcal{W}}\chi_2
\end{aligned} \tag{30}$$

where

$$\begin{aligned}
\chi_2 &= \begin{bmatrix}\chi_{21}\\ \chi_{22}\end{bmatrix}, \quad \mathcal{T}(t) = \begin{bmatrix}\bar{Z}_2 + T_1(t) & T_2(t)\\ (*) & \bar{Z}_2 + T_3(t)\end{bmatrix}, \\
T_1(t) &= (1-\alpha_d(t))X_1, \quad T_3(t) = \alpha_d(t)X_2, \\
T_2(t) &= \alpha_d(t)Y_1 + (1-\alpha_d(t))Y_2,
\end{aligned} \tag{31}$$

being X_1, X_2, Y_1, Y_2 matrices satisfying $\forall 0 \le \alpha_d(t) \le 1$:

$$\begin{bmatrix}\bar{Z}_2 & 0\\ 0 & \bar{Z}_2\end{bmatrix} - \alpha_d(t)\begin{bmatrix}X_1 & Y_1\\ (*) & 0\end{bmatrix} - (1-\alpha_d(t))\begin{bmatrix}0 & Y_2\\ (*) & X_2\end{bmatrix} \ge 0 \tag{32}$$

Therefore, we have from (26), (27) and (30) that

$$-\tau\int_{t-h_2}^{t-h_1}\dot{\xi}(s)^T Z_2\dot{\xi}(s)\leq -\chi_2^T\mathcal{T}(t)\chi_2 \tag{33}$$

Taking into account (27), (33) and (36), the time-derivative $\dot{V}$ in (37) can be bounded as:

$$\begin{aligned}\dot{V}\leq\ &\xi^T\Pi_0(t)\xi+He\left(\xi^T\Pi_1(t)\xi^T(t-h(t))\right)+He\left(\dot{\xi}_r^T\bar{R}\xi_r\right)\\&+\xi^TQ_1\xi-\xi^T(t-h_1)Q_1\xi(t-h_1)\\&+\xi^TQ_2\xi-\xi^T(t-h_2)Q_2\xi(t-h_2)\\&+\dot{\xi}^T\tilde{Z}\dot{\xi}-\chi_1^T\left(\mathcal{W}^T\bar{Z}_1\mathcal{W}\right)\chi_1-\chi_2^T\bar{\mathcal{W}}^T\mathcal{T}(t)\bar{\mathcal{W}}\chi_2\end{aligned} \tag{34}$$

where

$$\Pi_0(t)=\begin{bmatrix}\Omega_0(t) & 0\\ (*) & \Omega_0(t)\end{bmatrix},\quad \Pi_1(t)=\begin{bmatrix}\Omega_1(t) & \Omega_2(t)\\ \Omega_3(t) & \Omega_4(t)\end{bmatrix}$$

and

$$\begin{aligned}\Omega_0(t)&=\alpha\left(\gamma_1+\gamma_2cos(\phi-\theta)+\gamma_3sin(\phi-\theta)\right),\\ \Omega_1(t)&=-\frac{1}{2}K_ve^{\alpha h(t)}\left(\gamma_1+\gamma_2cos(\phi-\theta)+\gamma_3sin(\phi-\theta)\right),\\ \Omega_2(t)&=-\frac{1}{4}K_w\gamma_3e^{\alpha h(t)}\left(\frac{\rho_\alpha}{\rho_\alpha^{(h)}}\right),\\ \Omega_3(t)&=-\frac{1}{4}K_v\left(\gamma_2sin(\phi-\theta)+\gamma_3cos(\phi-\theta)\right)e^{\alpha h(t)},\\ \Omega_4(t)&=-\frac{1}{4}K_w\gamma_2e^{\alpha h(t)}\left(\frac{\rho_\alpha}{\rho_\alpha^{(h)}}\right).\end{aligned} \tag{35}$$

On the other hand, to deal with terms $\dot{\xi}$ and $\dot{\xi}_r$ in (34), note that time-derivative of (14) renders:

$$\begin{aligned}\dot{\xi}_1&=sat(v^{(h)})e^{\alpha t}+\alpha\rho_\alpha cos(\phi-\theta)-\rho_\alpha sin(\phi-\theta)sat(w^{(h)}),\\ \dot{\xi}_2&=\alpha\rho_\alpha sin(\phi-\theta)+\rho_\alpha sin(\phi-\theta)sat(w^{(h)}).\end{aligned} \tag{36}$$

Applying (22), (14) and (7), the above expression can be rewritten as:

$$\begin{aligned}\dot{\xi}_1&=-K_v\xi_1^{(h)}e^{\alpha h(t)}+\alpha\xi_1+K_w\xi_2sin\left(\phi^{(h)}-\theta^{(h)}\right),\\ \dot{\xi}_2&=\alpha\xi_2-K_w\xi_2sin\left(\phi^{(h)}-\theta^{(h)}\right).\end{aligned} \tag{37}$$

The above expression in compact form renders:

$$\dot{\xi}=\Pi_{21}(t)\xi(t)+\Pi_{22}(t)\xi(t-h(t)) \tag{38}$$

where $\Pi_{21}(t)$ and $\Pi_{22}(t)$ are defined as:

$$\Pi_{21}(t)=\begin{bmatrix}\alpha & \Omega_5(t)\\ 0 & \Omega_6(t)\end{bmatrix},\quad \Pi_{22}(t)=\begin{bmatrix}-K_ve^{\alpha h(t)} & 0\\ 0 & 0\end{bmatrix}$$

with

$$\begin{aligned}\Omega_5(t)&=K_wsin(\phi^{(h)}-\theta^{(h)}),\\ \Omega_6(t)&=\alpha-K_wsin(\phi^{(h)}-\theta^{(h)})\end{aligned} \tag{39}$$

Now, let us define the augmented state vector:

$$\begin{aligned}\bar{\xi}(t)=\Big[&\xi^T(t),\quad \xi^T(t-h(t)),\quad \xi^T(t-h_1),\quad \xi^T(t-h_2),\\ &\frac{1}{h_1}\int_{t-h_1}^{t}\xi^T(s)ds,\quad \frac{1}{h(t)-h_1}\int_{t-h(t)}^{t-h_1}\xi^T(s)ds,\\ &\frac{1}{h_2-h(t)}\int_{t-h_2}^{t-h(t)}\xi^T(s)ds\Big]^T\end{aligned} \tag{40}$$

Hence, we can write ξ, $\xi(t-h(t))$, ξ_r, $\dot{\xi}_r$, χ_1, χ_2 as a function of $\bar{\xi}\equiv\bar{\xi}(t)$ as:

$$\begin{aligned}&\xi=E_1\bar{\xi},\quad \xi(t-h(t))=E_2\bar{\xi},\\ &\dot{\xi}=\Pi_2(t)\bar{\xi},\quad \xi_r=\Pi_3(t)\bar{\xi},\quad \dot{\xi}_r=\Pi_4(t)\bar{\xi},\\ &\chi_1=\mathcal{D}_1\bar{\xi},\qquad \chi_2=\mathcal{D}_2\bar{\xi}\end{aligned} \tag{41}$$

where

$$\begin{aligned}\Pi_2(t)&=\Pi_{21}(t)E_1+\Pi_{22}(t)E_2,\\ \Pi_3(t)&=\left[E_1^T\quad h_1E_5^T\quad \tau\alpha_d(t)E_6^T+\tau(1-\alpha_d(t))E_7^T\right]^T,\\ \Pi_4(t)&=\left[\Pi_2^T(t)\ (E_1-E_3)^T\ (E_3-E_4)^T\right]^T.\end{aligned} \tag{42}$$

Therefore, we can write $\dot{V}(t)$ as

$$\begin{aligned}\dot{V}(t)=\bar{\xi}^T\Big[&E_1^T\Pi_0(t)E_1+He\left(E_1^T\Pi_1(t)E_2\right)\\&+He\left(\Pi_4^T(t)\bar{R}\Pi_3(t)\right)+E_1^TQ_1E_1-E_3^TQ_1E_3\\&+E_1^TQ_2E_1-E_4^TQ_2E_4\\&+\Pi_2^T(t)\tilde{Z}\Pi_2(t)-\mathcal{D}_1^T\mathcal{W}^T\bar{Z}_1\mathcal{W}\mathcal{D}_1\\&-\mathcal{D}_2^T\bar{\mathcal{W}}^T\mathcal{T}(t)\bar{\mathcal{W}}\mathcal{D}_2\Big]\bar{\xi}\end{aligned} \tag{43}$$

The stability condition with exponential decay rate α is satisfied if $\dot{V}<0$, which is equivalent to

$$\begin{bmatrix}\Pi(t) & \Pi_2^T(t)\tilde{Z}\\ (*) & -\tilde{Z}\end{bmatrix}<0 \tag{44}$$

where

$$\begin{aligned}\Pi(t)=\ &E_1^T\Pi_0(t)E_1+He\left(E_1^T\Pi_1(t)E_2\right)\\&+He\left(\Pi_4^T(t)\bar{R}\Pi_3(t)\right)+E_1^TQ_1E_1-E_3^TQ_1E_3\\&+E_1^TQ_2E_1-E_4^TQ_2E_4\\&-\mathcal{D}_1^T\mathcal{W}^T\bar{Z}_1\mathcal{W}\mathcal{D}_1-\mathcal{D}_2^T\bar{\mathcal{W}}^T\mathcal{T}(t)\bar{\mathcal{W}}\mathcal{D}_2\end{aligned} \tag{45}$$

Note that (44) contains the following nonlinear functions, that can be reformulated as:

$$\begin{aligned}cos(\phi-\theta)&=\mu_{11}(t)\hat{\delta}_{11}+\mu_{12}(t)\hat{\delta}_{12},\\ sin(\phi-\theta)&=\mu_{21}(t)\hat{\delta}_{21}+\mu_{22}(t)\hat{\delta}_{22},\\ sin(\phi^{(h)}-\theta^{(h)})&=\mu_{31}(t)\hat{\delta}_{31}+\mu_{32}(t)\hat{\delta}_{32},\\ \left(\frac{\rho_\alpha}{\rho_\alpha^{(h)}}\right)&=\mu_{41}(t)\hat{\delta}_{41}+\mu_{42}(t)\hat{\delta}_{42},\\ \alpha_d(t)&=\mu_{51}(t)\hat{\delta}_{51}+\mu_{52}(t)\hat{\delta}_{52},\\ e^{\alpha h(t)}&=\mu_{51}(t)\hat{\delta}_{61}+\mu_{52}(t)\hat{\delta}_{62}\end{aligned} \tag{46}$$

where

$$\mu_{11}=\frac{1}{2}\left(1-cos(\phi-\theta)\right),\qquad \mu_{12}=1-\mu_{11},$$

$$\mu_{21} = \frac{1}{2}\left(1 - sin(\phi - \theta)\right), \qquad \mu_{22} = 1 - \mu_{21},$$
$$\mu_{31} = \frac{1}{2}\left(1 - sin(\phi^{(h)} - \theta^{(h)})\right), \qquad \mu_{32} = 1 - \mu_{31},$$
$$\mu_{41} = \frac{\rho_\alpha/\rho_\alpha^{(h)} - 1}{e^{-\alpha h_2} - 1}, \qquad \mu_{42} = 1 - \mu_{41},$$
$$\mu_{51} = \alpha_d(t), \qquad \mu_{52} = 1 - \mu_{51},$$
$$\mu_{61} = \frac{e^{\alpha h_2} - e^{\alpha h(t)}}{e^{\alpha h_2} - e^{\alpha h_1}}, \qquad \mu_{62} = 1 - \mu_{61}. \quad (47)$$

Hence, we can write

$$\Omega_0(t) = \alpha \sum_{i=1}^{2}\sum_{j=1}^{2} \mu_{1i}\mu_{2j}\left(\gamma_1 + \gamma_2\hat{\delta}_{1i} + \gamma_3\hat{\delta}_{2j}\right),$$
$$\Omega_1(t) = -\frac{1}{2}K_v \sum_{i=1}^{2}\sum_{j=1}^{2}\sum_{p=1}^{2} \mu_{1i}\mu_{2j}\mu_{6p} \times \left(\gamma_1 + \gamma_2\hat{\delta}_{1i} + \gamma_3\hat{\delta}_{2j}\right)\hat{\delta}_{6p},$$
$$\Omega_2(t) = -\frac{1}{4}K_w\gamma_3 \sum_{m=1}^{2}\sum_{p=1}^{2} \mu_{4m}\mu_{6p}\hat{\delta}_{6p}\hat{\delta}_{4m},$$
$$\Omega_3(t) = -\frac{1}{4}K_v \sum_{i=1}^{2}\sum_{j=1}^{2}\sum_{p=1}^{2} \mu_{1i}\mu_{2j}\mu_{6p}\left(\gamma_2\hat{\delta}_{2j} + \gamma_3\hat{\delta}_{1i}\right)\hat{\delta}_{6p},$$
$$\Omega_4(t) = -\frac{1}{4}K_w\gamma_2 \sum_{m=1}^{2}\sum_{p=1}^{2} \mu_{4m}\mu_{6p}\hat{\delta}_{6p}\hat{\delta}_{4m},$$
$$\Omega_5(t) = K_w \sum_{k=1}^{2} \mu_{3k}\hat{\delta}_{k3}, \qquad \Omega_6(t) = \alpha - K_w \sum_{k=1}^{2} \mu_{3k}\hat{\delta}_{k3}, \quad (48)$$

and therefore

$$\Pi_0(t) = \sum_{i=1}^{2}\sum_{j=1}^{2} \mu_{1i}\mu_{2j}\hat{\Pi}_{0,ij},$$
$$\Pi_1(t) = \sum_{i=1}^{2}\sum_{j=1}^{2}\sum_{m=1}^{2}\sum_{p=1}^{2} \mu_{1i}\mu_{2j}\mu_{4m}\mu_{6p}\hat{\Pi}_{1,ijmp},$$
$$\Pi_2(t) = \sum_{k=1}^{2}\sum_{p=1}^{2} \mu_{3k}\mu_{6p}\hat{\Pi}_{2,kp}, \qquad \Pi_3(t) = \sum_{n=1}^{2} \mu_{5n}\hat{\Pi}_{3,n},$$
$$\Pi_4(t) = \sum_{k=1}^{2}\sum_{p=1}^{2} \mu_{3k}\mu_{6p}\hat{\Pi}_{4,kp}, \qquad \mathcal{T}(t) = \sum_{n=1}^{2} \mu_{5n}\hat{\mathcal{T}}_n. \quad (49)$$

The above inequality can equivalently be expressed as:

$$\sum_{i=1}^{2}\sum_{j=1}^{2}\sum_{k=1}^{2}\sum_{m=1}^{2}\sum_{n=1}^{2}\sum_{p=1}^{2} \mu_{1i}\mu_{2j}\mu_{3k}\mu_{4m}\mu_{5n}\mu_{6p} \times \begin{bmatrix} \hat{\Pi}_{ijkmnp} & \hat{\Pi}_{2,kp}^T\tilde{Z} \\ (*) & -\tilde{Z} \end{bmatrix} < 0, \quad (50)$$

Finally, noting that the auxiliary functions $\mu_{f1} = \mu_{f1}(t)$, $\mu_{f2} = \mu_{f2}(t)$, $f = 1, \ldots, 6$ given in (47) satisfy $0 \leq \mu_{f1} \leq 1$, $0 \leq \mu_{f2} \leq 1$ and $\mu_{f1} + \mu_{f2} = 1$, $\forall t \geq 0$. Hence, by the convex sum properties of (50), it can be seen that the fulfilment of the matrix inequalities given in the fourth line of (8) implies that (50) is true, leading to $lim_{t\to\infty}\bar{\xi} = 0$. By the definition of $\bar{\xi}$ and ξ_1, ξ_2 in (14), this last condition leads to $lim_{t\to\infty}\rho_\alpha = 0$ for any orientation error $\phi - \theta$, which guarantees the global exponential convergence with decay rate α in the sense of Definition 1, recalling that $\rho_\alpha = \rho e^{\alpha t}$.

C. PROOF OF NO INPUT SATURATION

First, it is trivial to see from (7) that $K_w < \bar{w}$ ensures that $w < \bar{w}$. To guarantee that v satisfies $v < \bar{v}$, $\forall t \geq 0$, we assume that the initial distance from the mobile robot to the target position is time-constant and known: $\rho(t <= 0) = \rho_0$, where ρ_0 is the initial distance. The initial orientation error, denoted as $\phi_0 - \theta_0$, is also assumed to be time-constant but not necessarily known. Hence, two conditions must be satisfied:

- The initial state vector $\xi_0 = [\xi_{10}, \quad \xi_{20}]^T$ at time instant $t \leq 0$ with

$$\xi_{10} = \rho_0 cos(\phi_0 - \theta_0), \qquad \xi_{20} = \rho_0 sin(\phi_0 - \theta_0) \quad (51)$$

must be contained into a circle of radius $\bar{\rho}_0$, which is true if

$$V_0 < \left(\frac{1}{\bar{\rho}_0^2}\right)\xi_0^T\xi_0, \qquad V_0 \equiv V|_{\rho=\rho_0,\phi=\phi_0,\theta=\theta_0,t=0} \quad (52)$$

taking into account that $\xi_{10}^2 + \xi_{20}^2 = \rho_0^2$. From (12) we have

$$V_0 = \frac{\gamma_1}{2}\rho_0^2 + \frac{\gamma_2}{2}\rho_0^2 cos(\phi_0 - \theta_0) + \frac{\gamma_3}{2}\rho_0^2 sin(\phi_0 - \theta_0) + \xi_{r0}^T\bar{R}\xi_{r0} + \int_{t-h_1}^{t} \xi_0^T(s)Q_1\xi_0(s)ds + h_1\int_{-h_1}^{0}\int_{t+s}^{t} \dot{\xi}_0^T(g)Z_1\dot{\xi}_0(g)dgds \quad (53)$$
$$+ \int_{t-h_2}^{t-h_1} \xi_0^T(s)Q_2\xi_0(s)ds + \tau\int_{-h_2}^{-h_1}\int_{t+s}^{t} \dot{\xi}_0^T(g)Z_2\dot{\xi}_0(g)dgds \quad (54)$$

Recalling that ξ_0 is time-constant $\forall t \leq 0$, then $\dot{\xi}_0(g) = 0$, $-h_2 \leq g \leq 0$, and the above expression is equivalent to

$$V_0 = \frac{\gamma_1}{2}\rho_0^2 + \frac{\gamma_2}{2}\rho_0^2 cos(\phi_0 - \theta_0) + \frac{\gamma_3}{2}\rho_\alpha^2 sin(\phi_0 - \theta_0) + \xi_{r0}^T\bar{R}\xi_{r0} + \int_{t-h_1}^{t} \xi_0^T(s)Q_1\xi_0(s)ds + \int_{t-h_2}^{t-h_1} \xi_0^T(s)Q_2\xi_0(s)ds, \quad (55)$$

where $\xi_{r0} = \left[\xi_0, \quad \int_{t-h_1}^{t} \xi_0(s)ds, \quad \int_{t-h_2}^{t-h_1} \xi_0(s)ds\right]^T$. Recalling again that $\xi_0(s) = 0, -h_2 \leq s \leq 0$ and considering the above expression, the inequality (52) renders:

$$\begin{aligned} V_0 = \xi_0^T \Big(& \sum_{i=1}^{2}\sum_{j=1}^{2} \beta_{1i}\beta_{2j}\hat{\Xi}_{ij} \\ & + R_1 + h_1^2 R_4 + \tau^2 R_6 + h_1\left(R_2 + R_2^T\right) \\ & + \tau\left(R_3 + R_3^T\right) + h_1\tau\left(R_5 + R_5^T\right) \\ & + h_1 Q_1 + \tau Q_2\Big)\xi_0 < \left(\frac{1}{\bar{\rho}_0^2}\right)\xi_0^T\xi_0, \end{aligned} \tag{56}$$

where

$$\beta_{11} = \frac{1}{2}\left(1 + cos\left(\phi_0 - \theta_0\right)\right), \qquad \beta_{12} = 1 - \beta_{11},$$
$$\beta_{21} = \frac{1}{2}\left(1 + sin\left(\phi_0 - \theta_0\right)\right), \qquad \beta_{22} = 1 - \beta_{21}.$$

The above inequality (56) holds if

$$\begin{aligned} & \sum_{i=1}^{2}\sum_{j=1}^{2} \beta_{1i}\beta_{2j}\big(\hat{\Xi}_{ij} + R_1 + h_1^2 R_4 \\ & + \tau^2 R_6 + h_1\left(R_2 + R_2^T\right) \\ & + \tau\left(R_3 + R_3^T\right) + h_1\tau\left(R_5 + R_5^T\right) \\ & + h_1 Q_1 + \tau Q_2\big) < \frac{1}{\bar{\rho}_0^2}. \end{aligned} \tag{57}$$

- The velocity must not reach $\bar{v}$ for all initial distances to the target position satisfying $\rho_0 \leq \bar{\rho}_0$ regardless of the initial orientation error $\phi_0 - \theta_0$. Provided that the condition given above is satisfied, we have to ensure that $v \leq \bar{v}$ for all system trajectories contained in the level set $V < 1$. Hence, the following condition is established:

$$(1 - V) + \lambda_d\left(v^T v - \bar{v}^2\right) < 0 \tag{58}$$

for any scalar λ_d. Choosing $\lambda_d = 1/\bar{v}^2$, we have that

$$-V + \frac{1}{\bar{v}^2} v^T v < 0 \tag{59}$$

Taking into account that $Z_1 > 0, Z_2 > 0$, from the structure of V in (12) it is true that

$$-V < -\xi_r^T\left(\sum_{i=1}^{2}\sum_{j=1}^{2} \mu_{1i}\mu_{2j}\Xi_{ij}\right)\xi_r. \tag{60}$$

Therefore, applying (60) and noting that $v^T v = \xi_1^T K_v^T K_v \xi_1 e^{-2\alpha t} < \xi_1^T K_v^T K_v \xi_1$, we have that

$$\begin{aligned} -V + \frac{1}{\bar{v}^2} v^T v < & -\xi_r^T\left(\sum_{i=1}^{2}\sum_{j=1}^{2} \mu_{1i}\mu_{2j}\Xi_{ij}\right)\xi_r \\ & + \frac{1}{\bar{v}^2}\xi_r^T \bar{K}_v^T \bar{K}_v \xi_r < 0. \end{aligned} \tag{61}$$

The inequality (61) is true $\forall \xi_r$ if

$$\sum_{i=1}^{2}\sum_{j=1}^{2} \mu_{1i}\mu_{2j}\left(-\Xi_{ij} + \frac{1}{\bar{v}^2}\bar{K}_v^T \bar{K}_v\right) < 0. \tag{62}$$

Applying Schur Complement, the above inequality is true if

$$\sum_{i=1}^{2}\sum_{j=1}^{2} \mu_{1i}\mu_{2j}\begin{bmatrix} \Xi_{ij} & \bar{K}_v^T \\ \bar{K}_v & \bar{v}^2 \end{bmatrix} > 0. \tag{63}$$

The fulfilment of both conditions (57) and (63) implies that if the initial distance to the target position is less or equal than ρ_0, then the velocity v does not exceed $\bar{v}$ for any $t \geq 0$. Finally, it is easy to see that the inequalities (57) and (63) hold if the two first inequalities depicted in (8) are true.

DISCLOSURE STATEMENT

No potential conflict of interest was reported by the author(s).

REFERENCES

[1] S. Rasoolinasab, S. Mobayen, A. Fekih, P. Narayan, and Y. Yao, "A composite feedback approach to stabilize nonholonomic systems with time varying time delays and nonlinear disturbances," *ISA Trans.*, vol. 101, pp. 177–188, Jun. 2020.

[2] R. Brocket, "Asymptotic stability and feedback stabilization," in *Differential Geometric Control Theory*, R. W. Brockett, R. S. Milman, and H. J. Sussman, Eds. Boston, MA, USA: Birkhiuser, 1983.

[3] J. Lu, S. Sekhavat, M. Xie, and C. Laugier, "Sliding mode control for nonholonomic mobile robot," in *Proc. Int. Conf. Control, Autom., Robot. Vis.*, 2000, pp. 1–6.

[4] Y. Xie, X. Zhang, W. Meng, S. Zheng, L. Jiang, J. Meng, and S. Wang, "Coupled fractional-order sliding mode control and obstacle avoidance of a four-wheeled steerable mobile robot," *ISA Trans.*, vol. 108, pp. 282–294, Feb. 2021.

[5] H. Zhang, B. Li, B. Xiao, Y. Yang, and J. Ling, "Nonsingular recursive-structure sliding mode control for high-order nonlinear systems and an application in a wheeled mobile robot," *ISA Trans.*, vol. 130, pp. 553–564, Nov. 2022.

[6] H. G. Tanner and K. J. Kyriakopoulos, "Discontinuous backstepping for stabilization of nonholonomic mobile robots," in *Proc. IEEE Int. Conf. Robot. Autom.*, vol. 4, May 2002, pp. 3948–3953.

[7] F. Pourboghrat and M. P. Karlsson, "Adaptive control of dynamic mobile robots with nonholonomic constraints," *Comput. Electr. Eng.*, vol. 28, no. 4, pp. 241–253, Jul. 2002.

[8] Z. Peng, S. Yang, G. Wen, A. Rahmani, and Y. Yu, "Adaptive distributed formation control for multiple nonholonomic wheeled mobile robots," *Neurocomputing*, vol. 173, pp. 1485–1494, Jan. 2016.

[9] S. Blažič and M. Bernal, "Trajectory tracking for nonholonomic mobile robots based on extended models," *IFAC Proc. Volumes*, vol. 44, no. 1, pp. 5938–5943, Jan. 2011.

[10] H. O. Wang and K. Tanaka, *Fuzzy Control Systems Design and Analysis: A Linear Matrix Inequality Approach*. Hoboken, NJ, USA: Wiley, 2004.

[11] X. Li and M. Wang, "Consensus control for wheeled mobile robots under input saturation constraint," *IEEE Access*, vol. 8, pp. 177125–177130, 2020.

[12] K. Gu, J. Chen, and V. L. Kharitonov, *Stability of Time-Delay Systems*. Berlin, Germany: Springer, 2003.

[13] V. L. Kharitonov and A. P. Zhabko, "Lyapunov–Krasovskii approach to the robust stability analysis of time-delay systems," *Automatica*, vol. 39, no. 1, pp. 15–20, 2003.

[14] H. Shao, G. Yuan, Z. Pang, and Q. Han, "Stability of networked control systems: A Lyapunov–Krasovskii functional plus approach," *ISA Trans.*, vol. 136, pp. 235–244, May 2023.

[15] S. Boyd, L. El Ghaoui, E. Feron, and V. Balakrishnan, *Linear Matrix Inequalities in System and Control Theory*. Philadelphia, PA, USA: SIAM, 1994.
[16] J. F. Sturm, "Using SeDuMi 1.02, a MATLAB toolbox for optimization over symmetric cones," *Optim. Methods Softw.*, vol. 11, nos. 1–4, pp. 625–653, Jan. 1999.
[17] P. Gahinet, A. Nemirovski, A. Laub, and M. Chilali, "The LMI control toolbox," in *Proc. 33rd IEEE Conf. Decis. Control*, Dec. 1995, pp. 2038–2041.
[18] X.-M. Zhang, Q.-L. Han, and X. Ge, "The construction of augmented Lyapunov–Krasovskii functionals and the estimation of their derivatives in stability analysis of time-delay systems: A survey," *Int. J. Syst. Sci.*, vol. 53, no. 12, pp. 2480–2495, Sep. 2022.
[19] C. Briat, "Convergence and equivalence results for the Jensen's inequality—Application to time-delay and sampled-data systems," *IEEE Trans. Autom. Control*, vol. 56, no. 7, pp. 1660–1665, Jul. 2011.
[20] A. Seuret and F. Gouaisbaut, "Wirtinger-based integral inequality: Application to time-delay systems," *Automatica*, vol. 49, no. 9, pp. 2860–2866, Sep. 2013.
[21] P. Park, W. I. Lee, and S. Y. Lee, "Auxiliary function-based integral inequalities for quadratic functions and their applications to time-delay systems," *J. Franklin Inst.*, vol. 352, no. 4, pp. 1378–1396, Apr. 2015.
[22] A. Seuret and F. Gouaisbaut, "Stability of linear systems with time-varying delays using Bessel–Legendre inequalities," *IEEE Trans. Autom. Control*, vol. 63, no. 1, pp. 225–232, Jan. 2018.
[23] P. Park, J. W. Ko, and C. Jeong, "Reciprocally convex approach to stability of systems with time-varying delays," *Automatica*, vol. 47, no. 1, pp. 235–238, Jan. 2011.
[24] L. S. Rizi, S. Mobayen, M. T. Dastjerdi, V. Ghaffari, A. Bartoszewicz, and W. Assawinchaichote, "LMI-based composite nonlinear feedback tracker for uncertain nonlinear systems with time delay and input saturation," *IEEE Access*, vol. 10, pp. 100489–100500, 2022.
[25] Y.-Q. Wu and Z.-G. Liu, "Output feedback stabilization for time-delay nonholonomic systems with polynomial conditions," *ISA Trans.*, vol. 58, pp. 1–10, Sep. 2015.
[26] Z.-G. Liu, Y.-Q. Wu, and Z.-Y. Sun, "Output feedback control for a class of high-order nonholonomic systems with complicated nonlinearity and time-varying delay," *J. Franklin Inst.*, vol. 354, no. 11, pp. 4289–4310, Jul. 2017.
[27] A. González, Á. Cuenca, J. Salt, and J. Jacobs, "Robust stability analysis of an energy-efficient control in a networked control system with application to unmanned ground vehicles," *Inf. Sci.*, vol. 578, pp. 64–84, Nov. 2021.
[28] B. Wang, S. Nersesov, and H. Ashrafiuon, "Formation regulation and tracking control for nonholonomic mobile robot networks using polar coordinates," *IEEE Control Syst. Lett.*, vol. 6, pp. 1909–1914, 2022.
[29] A. Zhang, D. Zhou, M. Yang, and P. Yang, "Finite-time formation control for unmanned aerial vehicle swarm system with time-delay and input saturation," *IEEE Access*, vol. 7, pp. 5853–5864, 2019.
[30] Y. Jia, Y. Jia, K. Gong, and W. Zheng, "Velocity-free formation control for omnidirectional mobile robots with input saturation," *IET Control Theory Appl.*, vol. 17, no. 10, pp. 1265–1282, Jul. 2023.
[31] Z. Miao, Y. Wang, and R. Fierro, "Cooperative circumnavigation of a moving target with multiple nonholonomic robots using backstepping design," *Syst. Control Lett.*, vol. 103, pp. 58–65, 2017.
[32] M. Vidyasagar, *Nonlinear Systems Analysis*. Philadelphia, PA, USA: SIAM, 2002.
[33] R. Carbonell, Á. Cuenca, V. Casanova, R. Pizá, and J. J. Salt Llobregat, "Dual-rate extended Kalman filter based path-following motion control for an unmanned ground vehicle: Realistic simulation," *Sensors*, vol. 21, no. 22, p. 7557, Nov. 2021.
[34] F. M. López-Rodríguez and F. Cuesta, "Andruino-A1: Low-cost educational mobile robot based on Android and Arduino," *J. Intell. Robotic Syst.*, vol. 81, no. 1, pp. 63–76, Jan. 2016.
[35] R. Amsters, E. Demeester, N. Stevens, Q. Lauwers, and P. Slaets, "Evaluation of low-cost/high-accuracy indoor positioning systems," in *Proc. Int. Conf. Adv. Sensors, Actuat., Metering Sens. (ALLSENSORS)*, Athens, Greece, 2019, pp. 24–28.

ANTONIO GONZÁLEZ-SORRIBES received the degree in telecommunications engineering and the Ph.D. degree in automation and industrial informatics from Universitat Politècnica de València (UPV), Spain, in 2001 and 2012, respectively. He was a Postdoctoral Researcher with the Laboratory of Industrial and Human Automation Control, Mechanical Engineering and Computer Science, CNRS, UMR 8201, Valenciennes, France, from 2013 to 2014. He is currently an Associate Professor with the Department of Systems Engineering and Automation, UPV. His research interests are within the broad area of time delay systems, robust control, networked control systems, multirobot systems, and process control applications.

RAFAEL CARBONELL received the bachelor's degree in informatics engineering and the master's degree in automation and industrial computing from Universitat Politècnica de València (UPV), Valencia, Spain, in 2018 and 2019, respectively, where he is currently pursuing the Ph.D. degree with the Systems Engineering and Control Department. He is also a Senior Research Technician with the Automatics and Industrial Informatics University Research Institute (ai2). His research interests include networked and event-triggered control systems, multirate control systems, and autonomous vehicles.

ANGEL CUENCA received the M.Sc. degree in computer science and the Ph.D. degree in control engineering from Universitat Politècnica de València (UPV), Valencia, Spain, in 1998 and 2004, respectively. He is currently an Associate Professor with the Systems Engineering and Control Department, UPV. He was a Visiting Scholar with Lund Institute of Technology, Lund, Sweden, in 2008; North Carolina State University, Raleigh, NC, USA, in 2012; the Eindhoven University of Technology, Eindhoven, The Netherlands, in 2014; and the University of California at Berkeley, Berkeley, CA, USA, in 2016 and 2018. He has coauthored more than 60 technical papers in journals and conferences. His research interests include networked and event-triggered control systems, multirate control systems, and autonomous vehicles.

JULIÁN SALT received the M.Sc. degree in industrial engineering and the Ph.D. degree in control engineering from Universitat Politècnica de València (UPV), in 1986 and 1992, respectively. Since 1987, he has been a Full Professor of automatic control with UPV, teaching a wide range of subjects in the area from continuous and discrete simulation to automation and programmable logic controller applications. He was a Visiting Scholar in multirate control of hard disk drives with UC Berkeley, USA. He is currently the Head of the Department of Systems Engineering and Control, UPV. He has been the director of eight Ph.D. dissertations. He has taken part in research projects funded by local industries, Spanish Government, and the European Science Foundation. He has coauthored more than 90 technical articles in journals and technical meetings. His research interests include non-conventionally sampled control systems and network-based control systems. His research activity is currently involved in network-based control energy saving.